Paper 254

©Civil-Comp Press, 2012
Proceedings of the Eleventh International Conference
on Computational Structures Technology,
B.H.V. Topping, (Editor),
Civil-Comp Press, Stirlingshire, Scotland

Analytical and Computational Perspectives of Multi-Scale Theory for Homogeneous, Laminated Composite, and Sandwich Beams and Plates

A. Tessler[1], M. Gherlone[2], D. Versino[2] and M. Di Sciuva[2]
[1] Structural Mechanics and Concepts Branch, NASA Langley Research Center Hampton VA, United States of America
[2] Aerospace Engineering Department, Politecnico di Torino, Italy

Abstract

This paper reviews the theoretical foundation and computational mechanics aspects of the recently developed shear-deformation theory, called the refined zigzag theory (RZT). The theory is based on a multi-scale formalism in which an equivalent single-layer plate theory is refined with a robust set of zigzag local layer displacements that are free of the usual deficiencies found in common plate theories with zigzag kinematics. In the RZT, first-order shear-deformation plate theory is used as the equivalent single-layer plate theory, which represents the overall response characteristics. Local piecewise-linear zigzag displacements are used to provide corrections to these overall response characteristics that are associated with the plate heterogeneity and the relative stiffnesses of the layers. The theory does not rely on shear correction factors and is equally accurate for homogeneous, laminated composite, and sandwich beams and plates. Regardless of the number of material layers, the theory maintains only seven kinematic unknowns that describe the membrane, bending, and transverse shear plate-deformation modes. Derived from the virtual work principle, RZT is well-suited for developing computationally efficient, C^0-continuous finite elements; formulations of several RZT-based elements are highlighted. The theory and its finite element approximations thus provide a unified and reliable computational platform for the analysis and design of high-performance load-bearing aerospace structures.

Keywords: laminated composites, sandwich structures, refined zigzag theory, multi-scale, inter-laminar damage, C^0-continuous finite elements.

1 Introduction

Lightweight and high-performance characteristics of advanced composite materials have spurred a wide range of application of these materials in military and civilian aircraft, aerospace vehicles, and naval and civil structures. To realize the full potential of composite structures for primary load-bearing components, further advances in structural design, analysis methods, and failure prediction and progressive damage methodologies are necessary.

A wide variety of modern civilian and military aircraft use relatively thick laminated composite and sandwich laminates for primary load-bearing structures. Such structures commonly undergo relatively pronounced design-critical transverse-shear deformations and, under certain conditions, thickness-stretch deformations. Fail-safe designs require accurate stress-analysis methods, particularly in the regions of stress concentration. Moreover, computationally efficient progressive damage analysis necessitates accurate modeling of the interlaminar damage modes such as delamination. For these reasons, structural theories that account for higher-order deformation effects have attracted much attention in recent years.

Recently, Tessler and co-authors presented an improved structural theory for beams and plates, labeled the Refined Zigzag Theory (RZT), that offers substantial analytic and computational advantages for the analysis of homogeneous, laminated composite, and sandwich laminates [1-5]. This new theory is based on a multi-scale approach in which an equivalent single-layer plate theory is used to represent the overall (*coarse*) plate response characteristics and through-the-thickness zigzag kinematics are used to model the local (*fine*) layer-level behavior. In particular, the RZT uses First-order Shear-Deformation Theory (FSDT) as the equivalent single-layer theory, and uses sets of piecewise linear continuous functions to model the local behavior of the layers comprising a plate. The zigzag kinematic framework enables sufficiently accurate and computationally efficient modeling of a wide range of homogeneous and heterogeneous laminates without the use of shear correction factors. Novel zigzag functions, derived *a priori* from constitutive relations without enforcing debilitating stress-equilibrium constraints, are responsible for overcoming several critical shortcomings of the earlier zigzag theories (refer to [1-5] for the literature reviews and pertinent discussions). The stress resultants are obtained from the equilibrium equations and, as a result, are physically consistent with their definitions based on Hooke's relations. The formulation, which maintains a fixed number of kinematic unknowns regardless of the number of material layers, does not enforce full continuity of the transverse shear stresses along material-layer interfaces, yet is robust. Using the principle of virtual work, equilibrium equations and consistent boundary conditions are derived in a variationally consistent manner. The variational framework, requiring relatively simple C^0-continuous kinematic interpolations, provides a convenient means for developing computationally efficient and robust finite elements.

The focus of this paper is to assess the current state of the art in the development of RZT and to highlight its recent advances in finite element analysis. To accomplish these objectives, this paper first reviews the theoretical foundation of RZT for laminated plates and highlights the essential aspects of the piecewise linear zigzag functions derived from transverse-shear constitutive relations. Related efforts of the zigzag-function enrichment using higher-order polynomials are also highlighted. In Section 2, the principle of virtual work is presented, which serves as the foundation for developing finite element approximations. Also highlighted in this section are (i) a simple and effective method of computing highly accurate interlaminar stresses, (ii) the unique modeling of homogeneous plates using the full kinematics of RZT, and (iii) a higher-order theory that includes odd and even zigzag kinematic terms in the inplane expansions and which also accounts for the thickness-stretch deformations. In Section 3, recent efforts to develop RZT-based finite element for laminated composite and sandwich beam, plate, and shell structures are discussed, focusing on their kinematic approximations, element nodal configurations, and modeling capabilities. In Section 4, finite element results for a laminated cylindrical shell undergoing large displacements are presented to demostrate the latest RZT-based shell modeling capability. Finally, conclusions are presented which highlight the salient features of RZT and the finite elements developed on its foundation.

2 Foundation of Refined Zigzag Theory (RZT)

Consider a multilayer composite plate of uniform thickness $2h$ that is composed of perfectly bonded orthotropic layers, labelled with superscript (k), where k=1,…, N; furthermore, the plate undergoes small-strain deformations under static loading while exhibiting negligible inertial effects (refer to Figure 1.) The inplane coordinates of the plate are defined by the vector $\mathbf{x} \equiv (x_1, x_2) \in S_m$, where S_m represents the set of points given by the intersection of the plate with the plane $z=0$ (the midplane); the symbolism $z \in [-h, h]$ denotes the domain of the through-the-thickness coordinate.

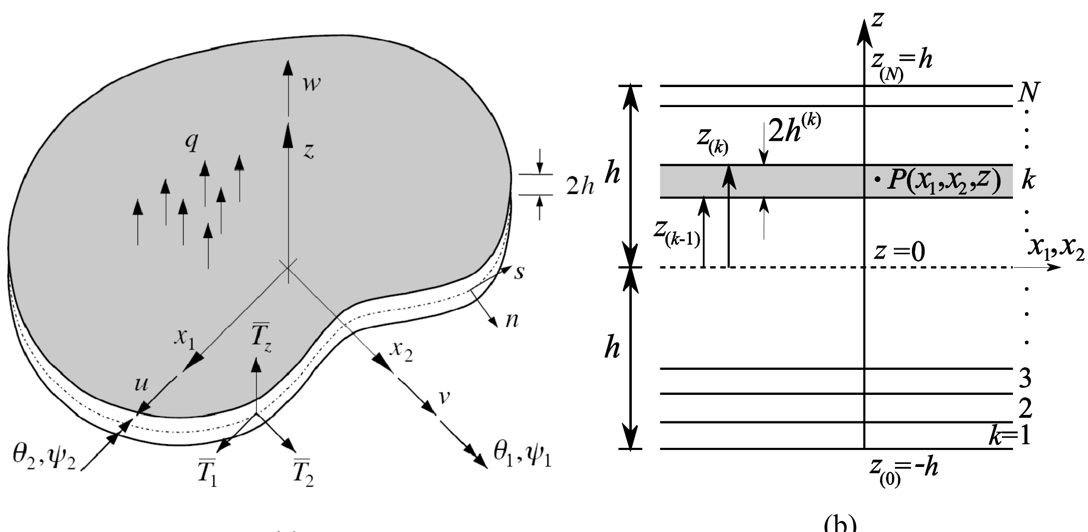

Figure 1. (a) Plate of uniform thickness, $2h$, subjected to transverse pressure loading, q, and edge tractions, $\{\overline{T}_\alpha \ (\alpha = 1,2)$, $\overline{T}_z\}$; (b) through-thickness notation of N-layer laminate.

The displacement vector of any material point $P(x_1, x_2, z)$ in the k^{th} layer is defined by the three orthogonal components $(u_1^{(k)}, u_2^{(k)}, u_z)$ that are expressed as [4-5],

$$
\begin{aligned}
u_1^{(k)}(\mathbf{x},z) &\equiv u(\mathbf{x}) + z\,\theta_1(\mathbf{x}) + \phi_1^{(k)}(z)\,\psi_1(\mathbf{x}) \\
u_2^{(k)}(\mathbf{x},z) &\equiv v(\mathbf{x}) + z\,\theta_2(\mathbf{x}) + \phi_2^{(k)}(z)\,\psi_2(\mathbf{x}) \\
u_z(\mathbf{x},z) &\equiv w(\mathbf{x})
\end{aligned}
\tag{1}
$$

where $u(\mathbf{x})$ and $v(\mathbf{x})$ are the inplane displacements in the x_1 and x_2 coordinate directions, respectively, and $w(\mathbf{x})$ is the transverse deflection. The symbols $\theta_1(\mathbf{x})$ and $\theta_2(\mathbf{x})$ represent overall bending rotations of a transverse material line element, that is initially straight and normal to the midplane, about the positive x_2 and the negative x_1 directions, respectively. These overall rotations represent linearized weighted averages of the actual nonlinear through-the-thickness displacement variations that are produced when the displacement variations within each layer are pronounced. Collectively, these three displacements and two rotations form the basis of FSDT and, as such, are viewed herein as the quantities that define the overall, first-approximation, coarse displacement characteristics of a plate.

Refinements to the coarse displacement characteristics, and hence improved fidelity, are obtained by introducing additional displacement functions that model lamina-scale, or even sub-lamina-scale, responses adequately. In the RZT, the refined contributions to the "coarse" inplane displacements are due to the zigzag terms $\phi_\alpha^{(k)}(z)\,\psi_\alpha(\mathbf{x})$ $(\alpha = 1,2)$ that appear in Eqs. (1). These refinement functions generally produce piecewise-continuous, nonlinear through-the-thickness distributions that are defined by the *zigzag* functions $\phi_\alpha^{(k)}(z)$ and their corresponding rotation (or amplitude) functions $\psi_\alpha(\mathbf{x})$. The simplest form for $\phi_\alpha^{(k)}(z)$ is given by a set of piecewise linear, continuous functions with derivatives $\phi_{\alpha,z}^{(k)}$ that are discontinuous at the layer interfaces. Herein, a comma followed by the subscript z denotes differentiation with respect to the through-the-thickness coordinate z. This particular class of functions is denoted herein by $C_z^{(0)}$.

The localized rotations of the line elements within each layer, which prior to deformation are straight and perpendicular to the reference midplane, are obtained from Eqs. (1) as

$$
u_{\alpha,z}^{(k)}\left(\mathbf{x},z\right) = \theta_\alpha\left(\mathbf{x}\right) + \beta_\alpha^{(k)}\;\psi_\alpha\left(\mathbf{x}\right) \quad (\alpha = 1,2)
\tag{2}
$$

where $\beta_\alpha^{(k)} \equiv \phi_{\alpha,z}^{(k)}$ are constant valued within the k^{th} layer and generally have different values for layers with different material properties; thus, they are discontinuous at the layer interfaces. Therefore, the rotations $u_{\alpha,z}^{(k)}(\mathbf{x},z)$ are also uniform within the k^{th} layer and generally vary from layer to layer.

A key step within RZT is to identify its relationship with FSDT. This task is accomplished by representing the *coarse* rotations, $\theta_\alpha(\mathbf{x})$, as the weighted-average rotations, i.e.,

$$\theta_\alpha(\mathbf{x}) \equiv \frac{1}{2h}\int_{-h}^{h} u_{\alpha,z}^{(k)}\left(\mathbf{x},z\right)dz \quad (\alpha=1,2) \tag{3}$$

Substituting Eq. (2) into (3), results in

$$\int_{-h}^{h} \beta_\alpha^{(k)}\, dz = \phi_\alpha^{(N)}(h) - \phi_\alpha^{(1)}(-h) = 0 \quad (\alpha=1,2) \tag{4}$$

thus guaranteeing equal values of the zigzag functions on the bounding surfaces, i.e., $\phi_\alpha^{(N)}(h) = \phi_\alpha^{(1)}(-h)$ $(\alpha=1,2)$. To correlate the displacement of FSDT and RZT at the bounding surfaces, $z=\pm h$, it becomes immediately apparent that the top and bottom values of the zigzag functions must vanish identically, i.e.,

$$\phi_\alpha^{(N)}(h) = \phi_\alpha^{(1)}(-h) = 0 \quad (\alpha=1,2) \tag{5}$$

Equations (3) also imply that the following weighted-average transverse shear strains are those which correspond to FSDT, i.e.,

$$\gamma_\alpha = \frac{1}{2h}\int_{-h}^{h} \gamma_{\alpha z}^{(k)} dz = w_{,\alpha} + \theta_\alpha \quad (\alpha=1,2) \tag{6}$$

where henceforth the notation $(\bullet)_{,\alpha} \equiv \partial(\bullet)/\partial x_\alpha$ denotes partial differentiation with respect to the midplane coordinate, x_α.

It can now be readily ascertained that within RZT only the *coarse* kinematic variables define the values of the inplane displacements at top and bottom surfaces, i.e.,

$$\begin{aligned} u_1^{(1)}(\mathbf{x},-h) &= u(\mathbf{x}) - h\,\theta_1(\mathbf{x}),\ u_1^{(N)}(\mathbf{x},h) = u(\mathbf{x}) + h\,\theta_1(\mathbf{x}) \\ u_2^{(1)}(\mathbf{x},-h) &= v(\mathbf{x}) - h\,\theta_2(\mathbf{x}),\ u_2^{(N)}(\mathbf{x},h) = v(\mathbf{x}) + h\,\theta_2(\mathbf{x}) \end{aligned} \tag{7}$$

With this insight, it becomes clear that the zigzag kinematics can indeed be regarded as local ply-level perturbations to the overall, coarse displacement fields. From Eqs. (7), the physical interpretations of the *coarse* variables $\{u,\ v,\ \theta_1,\ \theta_2\}$ in terms of the top-surface inplane displacements $u_{\alpha t}(\mathbf{x}) \equiv u_\alpha^{(N)}(\mathbf{x},h)$ and the bottom-surface inplane displacements $u_{\alpha b}(\mathbf{x}) \equiv u_\alpha^{(1)}(\mathbf{x},-h)$ also become apparent, i.e.,

$$u(\mathbf{x}) = \frac{1}{2}\left[u_{1t}(\mathbf{x}) + u_{1b}(\mathbf{x})\right],\ \theta_1(\mathbf{x}) = \frac{1}{2h}\left[u_{1t}(\mathbf{x}) - u_{1b}(\mathbf{x})\right] \tag{8}$$

$$v(\mathbf{x}) = \frac{1}{2}\left[u_{2t}(\mathbf{x}) + u_{2b}(\mathbf{x})\right],\ \theta_2(\mathbf{x}) = \frac{1}{2h}\left[u_{2t}(\mathbf{x}) - u_{2b}(\mathbf{x})\right] \tag{9}$$

These same relations hold for these kinematic variables used in FSDT.

For certain classes of problems, modelling advantages can be exploited by using a different set of primary unknown functions instead of the seven appearing in Eqs. (1). For example, in finite element analyses that use the sub-laminate concept [6-9], the inplane displacements of the top and bottom bounding surfaces of a sub-laminate are particularly useful as primary unknowns. Thus, by treating a laminate as a collection of contiguous sub-laminates, the RZT equations presented herein can be modified as follows. From Eqs. (8) and (9), it is seen that an alternate description of the RZT displacement fields is obtained by expressing the four *coarse* variables $\{u, v, \theta_1, \theta_2\}$ in terms of the four inplane displacements of the top and bottom surfaces $\{u_{\alpha t}(\mathbf{x}),\ u_{\alpha b}(\mathbf{x})\}$ $(\alpha = 1,2)$, and then substituting the result into Eqs. (1). In this way, RZT is redefined in terms of the alternative set of seven displacement variables: $\{u_{\alpha t}(\mathbf{x}),\ u_{\alpha b}(\mathbf{x}),\ \psi_\alpha(\mathbf{x}),\ w(\mathbf{x})\}$ $(\alpha = 1,2)$ which can be applied on a laminate and a sub-laminate level. Because this transformation of the primary unknowns is well defined, this version of RZT is expected to have the same analytic accuracy as the original RZT.

Using the linear strain-displacement relations of elasticity theory and the displacement assumptions given by Eqs. (1), the RZT strains are given as

$$
\begin{aligned}
\varepsilon_{11}^{(k)} &= u_{,1} + z\theta_{1,1} + \phi_1^{(k)}\psi_{1,1} \\
\varepsilon_{22}^{(k)} &= v_{,2} + z\theta_{2,2} + \phi_2^{(k)}\psi_{2,2} \\
\gamma_{12}^{(k)} &= u_{,2} + v_{,1} + z(\theta_{1,2} + \theta_{2,1}) + \phi_1^{(k)}\psi_{1,2} + \phi_2^{(k)}\psi_{2,1} \\
\gamma_{\alpha z}^{(k)} &= \gamma_\alpha + \beta_\alpha^{(k)}\,\psi_\alpha \quad (\alpha = 1,2)
\end{aligned}
\tag{10}
$$

where it is noted that the inplane strains, $\{\varepsilon_{11}^{(k)}, \varepsilon_{22}^{(k)},\ \gamma_{12}^{(k)}\}$, are piecewise linear through the laminate thickness. The transverse shear strains, $\gamma_{\alpha z}^{(k)}$, are <u>piecewise constant</u>, i.e., they are constant within each material layer but discontinuous along the layer interfaces, in contrast to those of FSDT which are constant across the total laminate thickness.

Each layer of the plates considered herein is presumed to be specially orthotropic with respect to a set of principal material coordinate directions. In addition, each set of layer principal material axes have two axes that reside in the plane of the layer and a third that is perpendicular to that plane. This third axis is parallel to the *z*-axis for the plate coordinates defined herein. The two principal axes that reside in the plane of the layer are generally noncoincident with the inplane coordinate axes of the plate. In terms of the plate coordinate system, the generalized Hooke's relations for the k^{th} layer are given herein by

$$
\begin{Bmatrix} \sigma_{11} \\ \sigma_{22} \\ \tau_{12} \end{Bmatrix}^{(k)} = \begin{bmatrix} C_{11} & C_{12} & C_{16} \\ & C_{22} & C_{26} \\ sym. & & C_{66} \end{bmatrix}^{(k)} \begin{Bmatrix} \varepsilon_{11} \\ \varepsilon_{22} \\ \gamma_{12} \end{Bmatrix}^{(k)} \quad \text{or} \quad \boldsymbol{\sigma}^{(k)} = \mathbf{C}^{(k)}\,\boldsymbol{\varepsilon}^{(k)}
\tag{11.1}
$$

for the inplane stresses and by

$$\begin{Bmatrix} \tau_{2z} \\ \tau_{1z} \end{Bmatrix}^{(k)} = \begin{bmatrix} Q_{22} & Q_{12} \\ sym. & Q_{11} \end{bmatrix}^{(k)} \begin{Bmatrix} \gamma_{2z} \\ \gamma_{1z} \end{Bmatrix}^{(k)} \quad \text{or} \quad \boldsymbol{\tau}^{(k)} = \mathbf{Q}^{(k)}\,\boldsymbol{\gamma}^{(k)} \tag{11.2}$$

for the transverse shear stresses. The symbols $C_{ij}^{(k)}$ and $Q_{ij}^{(k)}$ denote the transformed elastic-stiffness coefficients referred to the plate coordinate system. In RZT, these coefficients are also based on the presumption that the transverse-normal stresses are negligible.

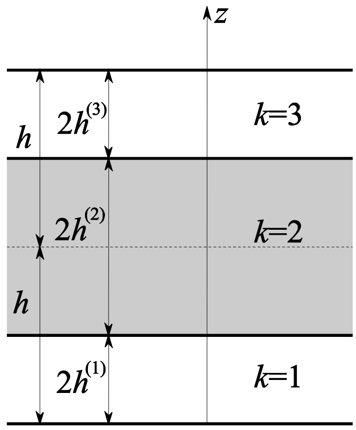

(a) Layer notation

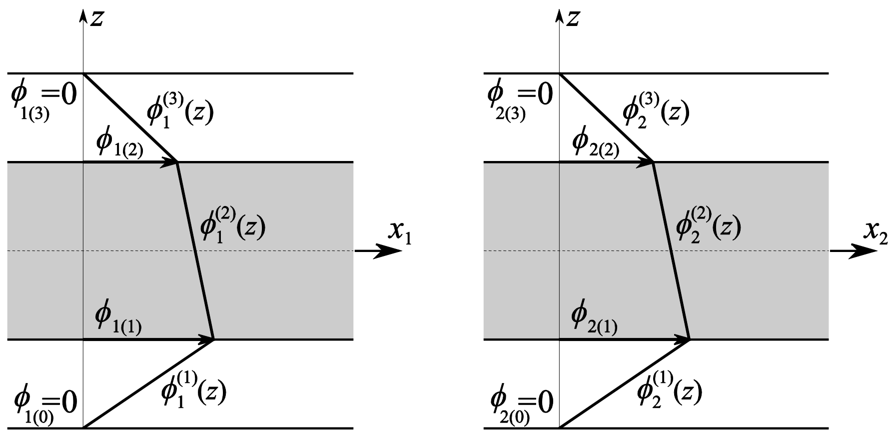

(b) Zigzag functions $\phi_1^{(k)}(z)$ and $\phi_2^{(k)}(z)$.

Figure 2. Notation for a three-layer laminate and $\phi_\alpha^{(k)}(z)$ zigzag functions defined in terms of interface displacements, $\phi_{\alpha(k)}$.

The next step in formulating RZT is to provide a mathematical description of the zigzag functions. Thus, for the k^{th} material layer, which is located in the range $[z_{(k-1)}, z_{(k)}]$, the zigzag functions are given as (see Figure 1(b) depicting the lamination notation),

$$\phi_{\alpha}^{(k)} \equiv \tfrac{1}{2}\left(1-\zeta^{(k)}\right)\phi_{\alpha(k-1)} + \tfrac{1}{2}\left(1+\zeta^{(k)}\right)\phi_{\alpha(k)} \quad (\alpha = 1,2) \tag{12.1}$$

where

$$\zeta^{(k)} \equiv \left[\left(z - z_{(k-1)}\right)/h^{(k)} - 1\right] \in \left[-1, 1\right] \quad \left(k = 1,\dots,N\right) \tag{12.2}$$

with the first layer, $k = 1$, beginning at $z_{(0)} = -h$, the last N^{th} layer, $k = N$, ending at $z_{(N)} = h$, and the k^{th} layer ending at $z_{(k)} = z_{(k-1)} + 2h^{(k)}$, where $2h^{(k)}$ denotes the k^{th} layer thickness. Evaluating Eqs. (12) at the bottom $(\zeta^{(k)} = -1)$ and top $(\zeta^{(k)} = 1)$ surfaces of the k^{th} layer, gives rise to the definitions of the interface displacements

$$\phi_{\alpha(k-1)} = \phi_{\alpha}^{(k)}(\zeta^{(k)} = -1), \quad \phi_{\alpha(k)} = \phi_{\alpha}^{(k)}(\zeta^{(k)} = 1) \quad \left(k = 1,\dots,N\right) \tag{13}$$

whereas according to Eqs. (5) the zigzag functions vanish at the bottom $(k = 1, \zeta^{(1)} = -1)$ and top $(k = N, \zeta^{(N)} = 1)$ plate surfaces, i.e., $\phi_{\alpha(0)} = \phi_{\alpha(N)} = 0$.

The remaining interface displacements can be obtained from the simple expression

$$\phi_{\alpha(k)} = \sum_{i=1}^{k} 2h^{(i)}\,\beta_{\alpha}^{(i)} \tag{14}$$

In [5], two alternative expressions have been derived for $\beta_{\alpha}^{(k)}$ $(k = 1,\dots,N-1)$; they are given as

$$\text{(a)} \quad \beta_{\alpha}^{(k)} = \frac{1}{\dfrac{Q_{\alpha\alpha}^{(k)}}{h}\displaystyle\sum_{k=1}^{N}\frac{h^{(k)}}{Q_{\alpha\alpha}^{(k)}}} - 1, \quad \text{(b)} \quad \beta_{\alpha}^{(k)} = \frac{S_{\alpha\alpha}^{(k)}}{\dfrac{1}{h}\displaystyle\sum_{k=1}^{N} h^{(k)} S_{\alpha\alpha}^{(k)}} - 1 \quad (\alpha = 1,2) \tag{15}$$

where $Q_{\alpha\alpha}^{(k)}$ and $S_{\alpha\alpha}^{(k)}$ $(\alpha = 1,2)$ denote, respectively, the diagonal transverse-shear stiffness and compliance coefficients of the k^{th} layer, respectively. Note that these expressions are only slightly different from each other for the general lay-up case, in which the transverse-shear constitutive matrix has a non-zero off-diagonal term ($Q_{12}^{(k)} \neq 0$). The two definitions, however, are identical for the special, decoupled case for which $Q_{12}^{(k)} = 0$. From the predictive perspective, either form of $\beta_\alpha^{(k)}$ yields excellent results, with the second form exhibiting slightly improved results, particularly for sandwich plates.

Further accuracy enhancements within the present RZT methodology can be achieved by using higher-degree polynomial expansions for the zigzag functions $\phi_\alpha^{(k)}$, that are piecewise continuous nonlinear functions, while keeping the basic kinematic assumptions, Eqs. (1), unchanged (e.g., refer to [10-13]).

2.1 Variational framework

The principle of virtual work, for the case of negligible body forces and zero shear tractions on the top and bottom bounding plate surfaces, may be written as

$$\begin{aligned}&\int_{S_m}\int_{-h}^{h}\left(\boldsymbol{\sigma}^{(k)T}\delta\boldsymbol{\varepsilon}^{(k)}+\boldsymbol{\tau}^{(k)T}\delta\boldsymbol{\gamma}^{(k)}\right)dz\,dS-\int_{S_m} q\,\delta w\,dS\\&-\int_{C_\sigma}\int_{-h}^{h}\left[\overline{T}_1\delta u_1^{(k)}+\overline{T}_2\delta u_2^{(k)}+\overline{T}_z\delta u_z\right]ds\,dz=0\end{aligned} \tag{16}$$

where δ is the variational operator; q is the applied transverse pressure attributed to the middle reference surface, S_m; $\{\overline{T}_\alpha\ (\alpha=1,2),\ \overline{T}_z\}$ are the inplane and transverse shear tractions that are prescribed along the cylindrical edge surface of the laminate, $S_\sigma \equiv C_\sigma \times s$. The bold-face vectors appearing in equation (16) are defined by Eqs. (11).

Integrating Eq. (16) across the laminate thickness, while accounting for the relationships in Eqs. (1) and (10), yields the corresponding two-dimensional statement of the principle of virtual work

$$\int_{S_m}[\mathbf{N}_m^T\delta\mathbf{e}_m+\mathbf{M}_b^T\delta\mathbf{e}_b+\mathbf{Q}_s^T\delta\mathbf{e}_s-q\delta w]\,dS-\int_{C_\sigma}\overline{\mathbf{F}}^T\delta\mathbf{u}\,ds=0 \tag{17.1}$$

where the membrane stress resultants and conjugate strain measures are defined as

$$\mathbf{N}_m^T\equiv\{N_1,N_2,N_{12}\}=\int_{-h}^{h}\{\sigma_{11}^{(k)},\sigma_{22}^{(k)},\tau_{12}^{(k)}\}dz,\ \ \mathbf{e}_m^T\equiv\{u_{,1},v_{,2},u_{,2}+v_{,1}\} \tag{17.2}$$

Likewise, the bending stress resultants and conjugate strain measures are defined as

$$\begin{aligned}\mathbf{M}_b^T&\equiv\left\{M_1,M_1^\phi,M_2,M_2^\phi,M_{12},M_{12}^\phi,M_{21}^\phi\right\}\\&=\int_{-h}^{h}\left\{z\,\sigma_{11}^{(k)},\phi_1^{(k)}\sigma_{11}^{(k)},z\,\sigma_{22}^{(k)},\phi_2^{(k)}\sigma_{22}^{(k)},z\,\tau_{12}^{(k)},\phi_1^{(k)}\tau_{12}^{(k)},\phi_2^{(k)}\tau_{12}^{(k)}\right\}dz\\\mathbf{e}_b^T&\equiv\left\{\theta_{1,1},\psi_{1,1},\theta_{2,2},\psi_{2,2},\theta_{1,2}+\theta_{2,1},\psi_{1,2},\psi_{2,1}\right\}\end{aligned} \tag{17.3}$$

The transverse shear stress resultants and conjugate strain measures are defined as

$$\mathbf{Q}_s^T \equiv \left\{Q_2, Q_2^\phi, Q_1, Q_1^\phi\right\} = \int_{-h}^{h} \left\{\tau_{2z}^{(k)}, \beta_2^{(k)}\,\tau_{2z}^{(k)}, \tau_{1z}^{(k)}, \beta_1^{(k)}\,\tau_{1z}^{(k)}\right\} dz$$

$$\mathbf{e}_s^T \equiv \left\{w_{,2} + \theta_2, \psi_2, w_{,1} + \theta_1, \psi_1\right\} \tag{17.4}$$

The force and moment resultants due to the prescribed tractions and their conjugate displacements are defined as

$$\begin{aligned}\bar{\mathbf{F}}^T &\equiv \{\bar{N}_{1n}, \bar{N}_{2n}, \bar{Q}_{zn}, \bar{M}_{1n}, \bar{M}_{2n}, \bar{M}_{1n}^\phi, \bar{M}_{2n}^\phi\} \\ &= \int_{-h}^{h} \{\bar{T}_1, \bar{T}_2, \bar{T}_z, z\bar{T}_1, z\bar{T}_2, \phi_1^{(k)}\bar{T}_1, \phi_2^{(k)}\bar{T}_2\} dz \qquad (17.5) \\ \mathbf{u}^T &\equiv \{u, v, w, \theta_1, \theta_2, \psi_1, \psi_2\}\end{aligned}$$

All elements of Eqs. (17) with the superscript ϕ are associated with the zigzag functions.

The stress resultants are readily obtained in terms of the two-dimensional plate strain measures by integrating the expressions in Eqs. (17) through the laminate thickness, resulting in the following constitutive relations of RZT:

$$\begin{Bmatrix}\mathbf{N}_m \\ \mathbf{M}_b \\ \mathbf{Q}_s\end{Bmatrix} = \begin{bmatrix}\mathbf{A} & \mathbf{B} & \mathbf{0} \\ \mathbf{B}^T & \mathbf{D} & \mathbf{0} \\ \mathbf{0} & \mathbf{0} & \mathbf{G}\end{bmatrix} \begin{Bmatrix}\mathbf{e}_m \\ \mathbf{e}_b \\ \mathbf{e}_s\end{Bmatrix} \tag{18}$$

where $\mathbf{A} \equiv [A_{ij}]_{3\times3}$ denotes the membrane stiffness matrix, $\mathbf{B} \equiv [B_{ij}]_{3\times7}$ is the membrane-to-bending coupling stiffness matrix, $\mathbf{D} \equiv [D_{ij}]_{7\times7}$ is the bending stiffness matrix, and $\mathbf{G} \equiv [G_{ij}]_{4\times4}$ is the transverse shear stiffness matrix. The explicit forms of these stiffness coefficients are found in [4,5]. Note that for a general composite lay-up, the membrane-to-bending coupling stiffnesses are nonzero; that is, $B_{ij} \neq 0$.

2.1.1 Special case

When the zigzag functions in the x_1 and x_2 directions are identical, $\phi_1^{(k)}(z) = \phi_2^{(k)}(z) \equiv \phi^{(k)}(z)$ $(k = 1,...,N)$. As a result, the two twisting moments associated with the zigzag kinematics are given by the same expression (refer to Eqs. (17.2) and [14]) as follows

$$M_{12}^\phi = M_{21}^\phi = \int_{-h}^{h} \phi^{(k)} \tau_{12}^{(k)} dz \tag{19}$$

This simplification gives rise to the following reduced form of Eqs. (17.2)

$$\begin{aligned}\mathbf{M}_b^T &\equiv \{M_1, M_2, M_{12}, M_1^\phi, M_2^\phi, M_{12}^\phi\} \\ &= \int_{-h}^{h} \{z\sigma_{11}^{(k)}, z\sigma_{22}^{(k)}, z\tau_{12}^{(k)}, \phi^{(k)}\sigma_{11}^{(k)}, \phi^{(k)}\sigma_{22}^{(k)}, \phi^{(k)}\tau_{12}^{(k)}\} dz \\ \mathbf{e}_b^T &\equiv \{\theta_{1,1}, \theta_{2,2}, \theta_{1,2}+\theta_{2,1}, \psi_{1,1}, \psi_{2,2}, \psi_{1,2}+\psi_{2,1}\}\end{aligned} \tag{20}$$

and the resulting simplifications in Eqs. (18). These constitutive relations provide a clear physical interpretation of the new quantities associated with the zigzag kinematics. Specifically, $\{M_1^\phi, M_2^\phi, M_{12}^\phi\}$ represent the bending and twisting moments due to the zigzag related cross-sectional distortions of the layers, whereas $\{\psi_{1,1}, \psi_{2,2}, \psi_{1,2}+\psi_{2,1}\}$ are their conjugate curvatures due to the normal zigzag rotations, ψ_1 and ψ_2.

2.2 Interlaminar stresses

An important attribute of any plate theory that is formulated to be robust at the local level is the ability to predict adequately interlaminar stresses that can be used to assess laminate failures. To provide adequate estimates of interlaminar stresses, it is often customary to integrate the three-dimensional equilibrium equations of elasticity theory. In this approach, the interlaminar transverse shear stresses are obtained by integrating the x_1 and x_2 derivatives of the inplane stresses

$$\begin{Bmatrix} \tau_{1z}^{(k)} \\ \tau_{2z}^{(k)} \end{Bmatrix} = -\int_{-h}^{z} \begin{Bmatrix} (\sigma_{11,1}^{(k)} + \tau_{12,2}^{(k)}) \\ (\sigma_{22,2}^{(k)} + \tau_{12,1}^{(k)}) \end{Bmatrix} dz \tag{21.1}$$

whereas the interlaminar transverse normal stresses are obtained by integrating the derivatives of the transverse shear stresses as

$$\sigma_{zz}^{(k)} = -\int_{-h}^{z} (\tau_{1z,1}^{(k)} + \tau_{2z,2}^{(k)})\, dz \tag{21.2}$$

Although this post-processing procedure has been widely advocated for use with FSDT and many higher-order theories, the adequacy of this scheme can be seen to be directly linked to (a) the accuracy of the inplane stresses obtained from constitutive relations of the underlying theory, and (b) the accuracy of the derivatives of these stresses (or second derivatives of the kinematic variables, refer to Eq. (10)), with this issue particularly relevant when finite element analyses are performed.

Regarding issue (a), it has been observed that FSDT and the vast majority of available structural theories often underestimate the inplane stresses; this is especially the case when highly heterogeneous and relatively thick laminates are analyzed, including the sandwich construction. Relative to issue (b), reasonably good improvements in estimating derivatives of the inplane stresses can be achieved by using smoothing techniques, e.g., [15].

Application of Eqs. (21), using RZT inplane stresses, has been shown to be highly effective, yielding accurate interlaminar stresses that are comparable to those predicted by three-dimensional elasticity. This robustness exists because the piecewise linear inplane stresses of RZT are consistently accurate, even for highly heterogeneous and relatively thick composite and sandwich laminates [1-5].

2.3 RZT modelling of homogeneous plates

The key property of a zigzag function is that it vanishes identically when the material has homogenous transverse shear properties across the total thickness. Consequently, when the zigzag terms vanish identically, the kinematic assumptions given by Eqs. (1) revert to those of FSDT, which require transverse shear correction factors. Tessler et al. [5] have found a simple and effective way to use the full power of RZT's kinematic field to model homogenous plate (and beam) problems, without the need for transverse shear correction factors. In this approach, a homogeneous plate is modelled as a multilayer heterogeneous laminate, in which the transverse shear moduli, $G_{\alpha 3}^{(k)} (\alpha = 1,2)$, vary only slightly from layer to layer, i.e.,

$$G_{\alpha 3}^{(k)} = G_{\alpha 3}\left(1+\varepsilon^{(k)}\right) \quad (\alpha = 1,2;\ k = 1,...,N) \tag{22.1}$$

where $G_{\alpha 3} \quad (\alpha = 1,2)$ denote the constant values of the shear moduli, and where

$$\varepsilon^{(k)} = \frac{s}{h^2}\left(z_{(k-1)}^2 + z_{(k)}^2 + z_{(k-1)} z_{(k)}\right) \ll 1 \quad (s \ll 1) \tag{22.2}$$

is a layerwise, dimensionless coefficient that is a function of the position of the k^{th} layer within the laminate thickness. Thus, since $\varepsilon^{(k)} \ll 1$ (e.g., by setting $s = 10^{-4}$), the values of $G_{\alpha 3}^{(k)}$ are only slightly perturbed compared to the constant shear-modulus values $G_{\alpha 3}$ of the corresponding homogeneous plate. Thus, in this approach, the homogeneous plate is replaced with a corresponding plate with an infinitesimal degree of heterogeneity, which for all practical purposes is homogeneous. This approach is effective even when the deviation from the constant value of the shear modulus of the homogeneous plate is less than 1/100 of a percent. The results in [5] have shown that as the number of material layers increases within this infinitesimally heterogeneous laminate, the solution approaches that of a homogeneous plate, exhibiting the well-known parabolic distribution of the transverse shear stresses across the plate thickness, as well as the cubic distribution of the inplane stresses, with the latter being particularly evident in relatively thick plates. Remarkably, the solution itself finds the correct transverse shear stress distributions, albeit in a piecewise constant manner, thus validating the lack of necessity for the transverse shear correction factors that are commonly used within FSDT and even within some theories of higher order.

2.4 Higher-order RZT including transverse normal deformations

The RZT presented herein incorporates FSDT as the underlying baseline plate theory that models the overall, coarse plate behavior. Thus, it follows that higher order RZT theories can be formulated by using other underlying baseline plate theories with the zigzag kinematics used herein or with zigzag kinematics of higher fidelity. For example, Barut et al. [14] combined an underlying {1,2}-order baseline theory, that uses an overall parabolic transverse displacement assumption, with piecewise quadratic RZT-based zigzag inplane displacements to obtain a higher-order refined zigzag plate with eleven kinematic variables; four more than the RZT presented herein. The displacement assumptions for this theory, labeled as RZT$^{\{2,2\}}$, are given as

$$
\begin{aligned}
u_1^{(k)}(\mathbf{x},z) &= u(\mathbf{x}) + z\theta_1(\mathbf{x}) + \phi_1^{(k)}(z)\psi_{11}(\mathbf{x}) + \frac{z}{h}\phi_1^{(k)}(z)\psi_{12}(\mathbf{x}) \\
u_2^{(k)}(\mathbf{x},z) &= v(\mathbf{x}) + z\theta_2(\mathbf{x}) + \phi_2^{(k)}(z)\psi_{21}(\mathbf{x}) + \frac{z}{h}\phi_2^{(k)}(z)\psi_{22}(\mathbf{x}) \\
u_z(\mathbf{x},z) &= w(\mathbf{x}) + \frac{z}{h}w_1(\mathbf{x}) + \left(\frac{z^2}{h^2} - \frac{1}{3}\right)w_2(\mathbf{x})
\end{aligned}
\tag{23}
$$

where $\phi_\alpha^{(k)}$ are the piecewise linear zigzag functions within the k^{th} layer, adopted from the original RZT formulation presented herein; $\psi_{\alpha 1}(\mathbf{x})$ and $\psi_{\alpha 2}(\mathbf{x})$ ($\alpha = 1,2$) are the four zigzag amplitudes that permit both non-symmetric, $\psi_{\alpha 1}(\mathbf{x})$, and symmetric, $\psi_{\alpha 2}(\mathbf{x})$, inplane zigzag deformation modes. In addition, an average transverse normal stress, σ_{zz}, is independently assumed as a cubic function through the laminate thickness, in the form proposed by Tessler [16]; that is

$$
\sigma_{zz}(\mathbf{x},z) = \sigma_{z0}(\mathbf{x}) + \sigma_{z1}(\mathbf{x})\left(\frac{z}{h} - \frac{z^3}{3h^3}\right) \tag{24.1}
$$

This representation of the normal through-the-thickness stress yields a parabolic expression for its derivative $\sigma_{zz,z}(\mathbf{x},z)$, given by

$$
\sigma_{zz,z}(\mathbf{x},z) = \frac{\sigma_{z1}(\mathbf{x})}{h}\left(1 - \frac{z^2}{h^2}\right) \tag{24.2}
$$

$$\sigma_{zz,z}(\mathbf{x}, z = \pm h) = 0 \tag{24.3}$$

Equations (24.3) constitute the exact conditions on σ_{zz} in the sense of three-dimensional equilibrium equations of elasticity theory for the case of zero-valued transverse-shear tractions on the bounding surfaces. The $\sigma_{z0}(\mathbf{x})$ and $\sigma_{z1}(\mathbf{x})$ terms in Eq. (24) are expressed in terms of kinematic variables of the theory by way of the least-square transverse strain compatibility relations originally proposed in [16].

Thus, in this new theory, both transverse shear and transverse normal (thickness-stretch) deformations are included. The present theory models accurately the in-plane and transverse stress components through the thickness. The addition of the even (symmetric) inplane zigzag modes, which are not included in the seven-variable RZT, contributes to some improvements of the inplane displacement, strain and stress response, with further improvements in the interlaminar transverse shear stresses. Furthermore, RZT$^{\{2,2\}}$ appears to be an excellent candidate for developing efficient and accurate C^0-continuous finite elements.

3 Finite element approximations

The variational statement given by Eq. (17.1) can be integrated by parts to produce a consistent set of equilibrium equations and boundary conditions, resulting in seven partial differential equilibrium equations in terms of seven kinematic variables [4-5]. The equilibrium equations can be solved exactly or approximately depending on the complexity of the material lay-up, boundary conditions, and loading. Refer to [1-5] for details of analytic and approximate solutions of simply supported and cantilevered beams and plates made of laminated composite and sandwich construction.

Alternatively, to enable large-scale analysis of complex aerospace structures, the variational statement, Eq. (17.1), can be discretized using finite elements. As in FSDT, the strain measures within RZT are given as first-order partial derivatives. The direct implication is that computationally efficient C^0-continuous beam, plate, and shell finite elements can be developed, and that the legacy finite element technology that has been developed for FSDT can also be used with RZT.

3.1 RZT beam elements

Recently, Gherlone et al. [17,18] and Onate et al. [19] derived planar beam finite elements based on the RZT beam formulation in Tessler et al. [1]. When the beam deformations are restricted only to the x_1-z plane, the second equation in Eqs. (1) is identically zero, and the theory reduces to the two displacement components, $u_1^{(k)}$ and u_z. Consequently, there remain four independent kinematic variables, $u(x_1)$, $w(x_1)$, $\theta_1(x_1)$, and $\psi_1(x_1)$, that describe the membrane, bending, transverse shear, and zigzag deformations.

Gherlone et al. [17,18] derived several low-order RZT beam finite elements with the aim of achieving the best compromise between accuracy and computational efficiency. The four kinematic variables use the *anisoparametric* (aka *interdependent*) interpolations, where the polynomial degree of $w(x_1)$ is one order higher than those approximating the $u(x_1)$, $\theta_1(x_1)$, and $\psi_1(x_1)$ variables. Such interpolation strategy enables free of shear locking element behaviour for slender beams. With an initial assumption of a parabolic distribution for $w(x_1)$, the authors explored several shear-related constraint conditions that gave rise to two-node elements and a coupled form for the $w(x_1)$ interpolation. The constraint condition requiring a constant variation of the transverse shear force gave rise to a remarkably accurate two-node beam element. For further details of this formulation and for elastostatic solutions of simply supported and cantilevered beams of various slenderness ratios and lamination properties, the reader is referred to [18].

Onate et al. [19] derived a two-node, RZT beam finite element using linear, isoparametric interpolations for the four kinematic variables, $u(x_1)$, $w(x_1)$, $\theta_1(x_1)$, and $\psi_1(x_1)$. To achieve an element capable of modelling slender beams without incurring the shear locking effect, the authors used reduced integration (a one point Gaussian quadrature rule) of the transverse-shear strain energy of the beam element. One of the most interesting numerical solutions presented was for a laminated beam with an imbedded delamination that was modeled as a compliant layer. It was shown that the RZT beam element is computationally efficient and is capable of high-fidelity modelling of imbedded delaminations.

3.2 RZT plate and shell elements

Versino et al. [20,21] developed six- and three-node triangular RZT-based plate finite elements. Adopting linear shape functions for the in-plane displacements, bending rotations, and zigzag amplitudes, and a quadratic shape function for the transverse deflection, (i.e., using the Tessler-Hughes anisoparametric interpolation strategy [22]), the element interpolations in terms of the linear area-parametric coordinates L_i have the form

$$\begin{aligned}
&u(x_1,x_2)=\sum_{i=1}^{3}u_iL_i,\ v(x_1,x_2)=\sum_{i=1}^{3}v_iL_i,\ w(x_1,x_2)=\sum_{k=1}^{6}w_kP_k\\
&\theta_1(x_1,x_2)=\sum_{i=1}^{3}\theta_{1i}L_i,\ \theta_2(x_1,x_2)=\sum_{i=1}^{3}\theta_{2i}L_i\\
&\psi_1(x_1,x_2)=\sum_{i=1}^{3}\psi_{1i}L_i,\ \psi_2(x_1,x_2)=\sum_{i=1}^{3}\psi_{2i}L_i
\end{aligned}\tag{25}$$

where $i\in\{1,2,3\}$ is an index ranging over the three corner nodes; $k\in\{1,m_{12},2,m_{23},3,m_{31}\}$ ranges over the corner and mid-edge nodes; and P_k defines the standard set of quadratic shape functions (see the nodal configurations in Figure 3.) The element topology includes six nodes; however, the mid-edge nodes have only degrees-of-freedom (dof) associated with the transverse deflection. Using these interpolations, the six-node element, called unconstrained, is readily derived by introducing Eqs. (25) in the variational principle, Eq. (17), while carrying out the necessary matrix and variational operations to obtain the element stiffness equations.

In addition, the authors derived a three-node, constrained anisoparametric element whose interpolation functions for the deflection variable in Eqs. (25) are constrained by suitable edge constraints, analogous to those which have been explored by Tessler and Hughes [22] for plates modeled with FSDT, and by Gherlone et al. [17,18] for beams modeled with RZT. The explicit edge-constraint procedure enforces the mid-edge w dof to be dependent on the corner-node dof of the rotation variables of the corresponding edges. By imposing one-dimensional constraint relations, requiring the two shear strain measures to be constant along the element edges, there results a coupled-form, parabolic deflection that is compatible along the element edges given by [21]

$$w(x_1,x_2)=\sum_{i=1}^{3}L_i w_i+\sum_{i=1}^{3}\left[\left(\theta_{1i}+c\psi_{1i}\right)L_{1i}+\left(\theta_{2i}+c\psi_{2i}\right)L_{2i}\right] \tag{26.1}$$

with

$$\begin{aligned}&L_{1i}\equiv\frac{L_i}{2}(b_k L_j-b_j L_k),\ L_{2i}\equiv\frac{L_i}{2}(a_j L_k-a_k L_j)\\&a_i\equiv x_{1k}-x_{1j},\ b_i\equiv x_{2j}-x_{2k}\end{aligned} \tag{26.2}$$

where the subscripts are given by the cyclic permutation of $i\in\{1,2,3\}$, $j\in\{2,3,1\}$, and $k\in\{3,1,2\}$; and where c is either 0 or -1, depending on the constraint strategy used in the element formulation.

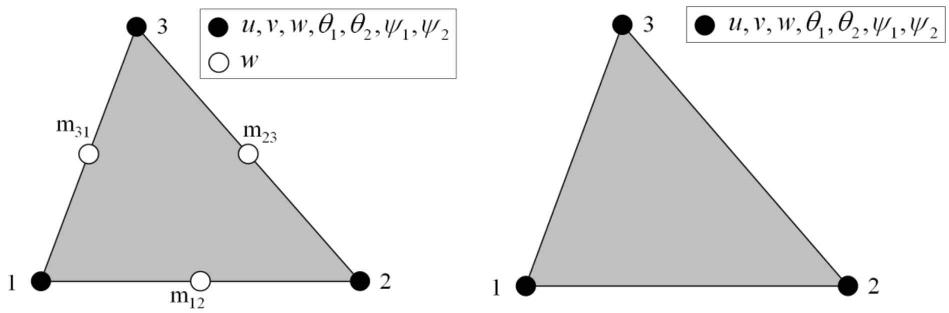

Figure 3. Six-node (unconstrained) and three-node (constrained) RZT-based anisoparametric plate elements.

An extensive numerical study was carried out in [21] on various laminated composite and sandwich plates undergoing elasto-static deformations. The results of this study demonstrate that the RZT-based anisoparametric elements possess superior accuracy and excellent convergence characteristics over a wide range of the span-to-thickness ratio. In addition, it was shown that the three-node elements provide the best compromise between computational efficiency and accuracy. Furthermore, the RZT models provide superior through-the-thickness predictions of the inplane and interlaminar stresses over comparable FSDT models, especially for relatively thick and highly heterogeneous laminated plate and sandwich plate constructions.

The latest finite element implementation of RZT, by Versino [23], is focused on developing robust anisoparametric shell finite elements that include the drilling dof (i.e., the dof associated with a rotation about the normal to the element's planar surface) and geometrically nonlinear deformations. In the next section, the application of RZT to an elastic cylindrical shell undergoing large displacements under quasi-static loading is demonstrated.

4 Nonlinear deformations of a laminated cylindrical shell

In this demonstration problem, a cylindrical shell is subjected to a quasi-static concentrated force, F, applied at point C (Figure 4). The global shell dimensions are L=254 mm, r=2540 mm, and θ=0.1 rad. The shell wall is a three-layer laminate with a total thickness $2h$=24 mm and with each layer having the same thickness. The prescribed boundary conditions are such that the straight edges are fully clamped and the curved edges are free. The mechanical material properties of isotropic material layers A and B are summarized in Table 1, and the laminate stacking sequence is given by [A/B/A]. Note that the elastic modulus of the middle layer is two orders of magnitude less than those of the top and bottom layers. This aspect, typical of sandwich construction, presents a significant challenge for any structural theory, since the through-the-thickness distributions of the inplane displacements exhibit interface slope discontinuities that are not accounted for in most structural theories.

To establish a viable reference solution for this problem, a high-fidelity, three-dimensional geometrically nonlinear FEM analysis was performed using the ABAQUS commercial code [24]. Depicted in Figure 4(a) is an FEM model which is arrived at from a convergence study. The model is based on C3D20 brick elements, discretizing a symmetric quadrant of the shell, using a 64x64x6 mesh (64 elements along each edge and 2 elements across the thickness of each layer). In addition, two shell-based geometrically nonlinear solutions were obtained: (a) an ABAQUS solution using the S3 (three-node, FSDT) shell elements, and (b) an RZT-based solution using RZT3 – a three-node anisoparametric element with drilling dof. Both shell models are based on the 32x32 mesh subdivisions that span the shell's symmetric quadrant, as shown in Figure 4(b).

Comparisons of the three nonlinear FEM solutions are shown in terms the load-deflection curve at point C in Figure 5. It is evident from these results that the three-dimensional FEM solution and the corresponding RZT3 solution are in very close agreement over the entire range of the applied loading. In contrast, the S3-model predictions are considerable less accurate, particularly over the range of larger displacements.

Material	Young's modulus, E (MPa)	Poisson ratio, ν
A	31×10^{2}	0.3
B	31	

Table 1. Mechanical material properties for isotropic layers.

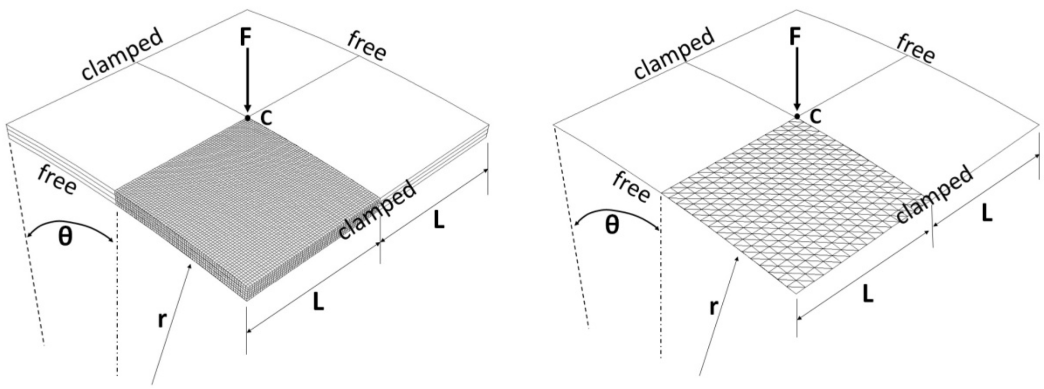

(a) Solid model (b) Shell model

Figure 4. Finite element discretization for cylindrical shell.

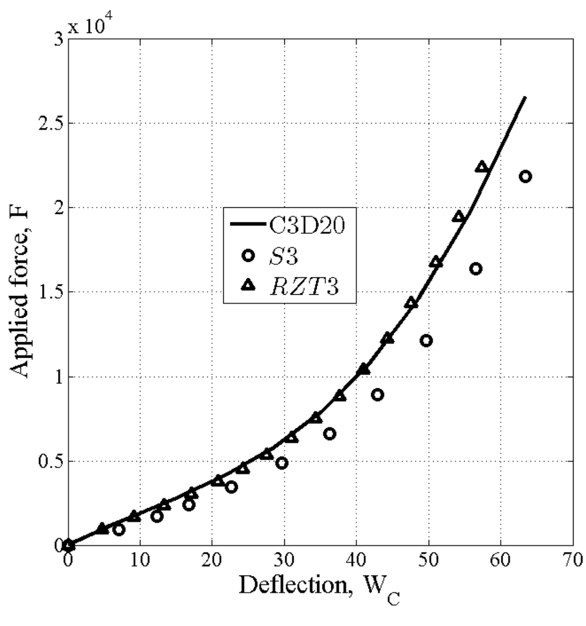

Figure 5. Applied force vs. deflection at point C.

5 Conclusions

In this paper the latest advances in the development of a shear-deformable, refined zigzag theory (RZT) for homogeneous, laminated composite, and sandwich beams and plates have been reviewed and the salient features highlighted. This theory maintains four kinematic unknowns for beams and seven for plates, regardless of the number of layers, material composition, or layer stacking sequence. In addition, it has been shown that the theory can be expressed in terms of displacement quantities that are amenable to sub-laminate modelling techniques. A higher-order plate theory that incorporates the RZT presented herein has also been described, which includes the thickness-stretch deformations in addition to the transverse shear deformations, and has eleven kinematic variables. This higher-order theory illustrates how the basic RZT presented herein can be adapted to obtain results with a very high degree of fidelity.

Analytic and computational aspects of the RZT and several new finite elements for beams, plates, and shells have also been highlighted. The unique characteristics of RZT and its finite elements is that they permit efficient modelling of a wide range of problems including homogenous beams and plates, composite laminates, sandwich construction, and compliant-layer delamination modelling. Such solutions do not require shear correction factors or any increase in model complexity or computational effort. In addition, RZT-based finite elements are amenable to much of the legacy finite element technology, especially that for FSDT-based elements. Because of these attributes, RZT has considerable promise for becoming the theory of choice for many practical applications including the computationally challenging problems of progressive damage modelling in composite structures.

Acknowledgements

The authors would like to express deep appreciation to Dr. Michael Nemeth, NASA Langley Research Center, and Prof. Erdogan Madenci and Dr. Atila Barut, University of Arizona, for their involvement in technical discussions and their thorough editorial review of this paper.

References

[1] A. Tessler, M. Di Sciuva, and M. Gherlone, "A refined zigzag beam theory for composite and sandwich beams", Journal of Composite Materials, 43(9), 1051-1081, 2009.

[2] M. Di Sciuva, M. Gherlone, and A. Tessler, "A robust and consistent first-order zigzag theory for multilayered beams", In Advances in Mathematical Modelling and Experimental Methods for Materials and Structures: The Jacob Aboudi Volume (Eds. R. Gilat, L. Banks-Sills) Springer (USA), ISBN, 255-268, 2009.

[3] A. Tessler, M. Di Sciuva, and M. Gherlone, "Recent advances toward computationally desirable zigzag bending theories for laminated composite

and sandwich plates", 13^{th} Conference on the Mathematics of Finite Elements and Applications Brunel University (MAFELAP), UK, 9 - 12 June, 2009 (keynote lecture).

[4] A. Tessler, M. Di Sciuva, and M. Gherlone, "A consistent refinement of first-order shear-deformation theory for laminated composite and sandwich plates using improved zigzag kinematics", Journal of Mechanics of Materials and Structures, 5(2), 341-367, 2010.

[5] A. Tessler, M. Di Sciuva, and M. Gherlone, "A homogeneous limit methodology and refinements of computationally efficient zigzag theory for homogeneous, laminated composite, and sandwich plates", Numerical Methods for Partial Differential Equations, 27(1), 208-229, 2011.

[6] Y. B. Cho and R. C. Averill, "First-order zig-zag sublaminate plate theory and finite element model for laminated composite and sandwich panels", Composite Structures, 50, 1-15, 2000.

[7] M. Di Sciuva and M. Gherlone, "A global/local third-order Hermitian displacement field with damaged interfaces and transverse extensibility: FEM formulation", Composite Structures, 59(4), 433-444, 2003.

[8] M. Gherlone and M. Di Sciuva, "Thermo-mechanics of undamaged and damaged multilayered composite plates: a sub-laminates finite element approach", Composite Structures, 81(1), 125-136, 2007.

[9] M. Gherlone and M. Di Sciuva, "Thermo-mechanics of undamaged and damaged multilayered composite plates: assessment of the FEM sub-laminates approach", Composite Structures, 81(1), 137-155, 2007.

[10] M. Di Sciuva, "Multilayered anisotropic plate models with continuous interlaminar stresses", Composite Structures, 22(3), 149 – 167, 1992.

[11] M. Di Sciuva, M. Gherlone, and L. Librescu, "Implications of damaged interfaces and of other non-classical effects on the load carrying capacity of multilayered composite shallow shells", International Journal of Non-Linear Mechanics, 37, 851-867, 2002.

[12] M. Gherlone, "Refinement of cubic zigzag: preliminary results", NASA-NIA (National Institute of Aerospace) Lecture, August 2007.

[13] M. P. Nemeth, "Cubic zig-zag enrichment of the classical Kirchhoff kinematics for laminated and sandwich plates", NASA-TM, 2012.

[14] A. Barut, E. Madenci, and A. Tessler, "A refined zigzag theory for laminated composite and sandwich plates incorporating thickness stretch deformation", Proceedings of AIAA/SDM Conference, 2012.

[15] A. Tessler and H. R. Riggs, "Accurate interlaminar stress recovery from finite element analysis", NASA-TM 109149, 1994.

[16] A. Tessler, "An improved plate theory of {1,2}-order for thick composite laminates", International Journal of Solids and Structures, 30, 981–1000, 1993.

[17] M. Gherlone, A. Tessler, and M. Di Sciuva, "A C^0-continuous two-node beam element based on refined zigzag theory and interdependent interpolation", MAFELAP 2009 Conference, Brunel University, London (UK), June 2009.

[18] M. Gherlone, A. Tessler, and M. Di Sciuva, "C^0 beam elements based on the refined zigzag theory for multilayered composite and sandwich laminates. Composite Structures, 93, 2882-2894, 2011.
[19] E. Oñate, A. Eijo, and S. Oller, "Simple and accurate two-noded beam element for composite laminated beams using a refined zigzag theory", Comput. Methods Appl. Mech. Engrg., 213-216, 362-382, 2012.
[20] D. Versino, M. Mattone, M. Gherlone, A. Tessler, and M. Di Sciuva, "An efficient, C -continuous triangular element for laminated composite and sandwich plates with improved zigzag kinematics", MAFELAP 2009 Conference, Brunel University, London (UK), June 2009.
[21] D. Versino, M. Gherlone, M. Mattone, M. Di Sciuva, and A. Tessler, "C^0 triangular elements based on the refined zigzag theory for multilayered composite and sandwich plates", Composites: Part B (to appear, 2012).
[22] A. Tessler and T. J. R. Hughes, "A three-node Mindlin plate element with improved transverse shear", Comput. Methods Appl. Mech. Engrg., 50, 71–101, 1985.
[23] D. Versino, "Refined theories and discontinuous Galerkin methods for the analysis of multilayered composite structures", Ph.D. thesis, Politecnico di Torino, Italy, 2012.
[24] ABAQUS/Standard User's Manual, Version 6.10, Dassault Systems Simulia Corp., Providence, RI, 2011.